Simulations and experiments on resonantly-pumped single-frequency Erbium lasers at 1.6 µm

A. Meissner[*a], P. Kucirek[a], J. Li[b], S. Yang[b], M. Hoefer[a], D. Hoffmann[a],
[a]Fraunhofer Institute for Laser Technology, Steinbachstr. 15, 52074 Aachen, Germany;
[b]School of Optoelectronics, Beijing Institute of Technology, Beijing 100081, China

ABSTRACT

We report on a single-frequency laser oscillator based on a new Er:YLuAG laser crystal which is spectrally suitable for application as a transmitter in differential absorption lidar measurements of atmospheric CH_4. The laser emits single-frequency laser pulses with 2.3 mJ of energy and 90 ns duration at a repetition rate of 100 Hz. It is resonantly pumped by two linearly polarized single-mode cw fiber lasers at 1532 nm. A scan of the CH_4-absorption line at 1645.1 nm was performed and the shape of the line with its substructure was reproduced as theoretically predicted. A 2.5-dimensional performance model was developed, in which pump absorption saturation and laser reabsorption is included. Also the spectral output of the laser oscillator longitudinal multimode operation could be predicted by the laser model.

Keywords: Erbium laser, single frequency, Lidar, q-switch, mixed garnet, quasi-three-level laser

1. INTRODUCTION

Knowledge of sources and sinks for climate gases is essential for understanding of atmospheric processes and modeling and prediction of climatic developments. In order to obtain this knowledge, long-term and global data on gas abundances are required, which can only be acquired with airborne and spaceborne detection systems. Lidar-Systems are favourable because they allow data acquisition at all times and weathers. Transmitters of these Lidar-Systems need single-frequency ("SF") laser beam sources at defined and specific central wavelengths. After Carbon Dioxide, Methane (CH_4) is the greenhouse gas with the second largest impact on the climate (measured as "radiative forcing" by IPCC). [1]
An appropriate wavelength pair for measuring CH4 with a differential absorption Lidar is around 1645.2 nm in air (1645.097 nm online, 1645.391 nm offline), which is also used in the French-German mission MERLIN [2]. Direct generation of such laser radiation in a tailor-made laser crystal without using non-linear frequency conversion has proven to enable higher spectral purity and lower beam propagation factors M² ([3]), requires a simpler setup and potentially provides higher efficiency than state-of-the art OPO-systems.
In this paper, a resonantly-pumped SF Q-switched laser oscillator based on an Er:YLuAG crystal as gain medium is presented. A performance model is described and compared to the measured results from the laser. Particularly the spectral properties of the laser oscillator were studied and eventually the CH_4-absorption line at 1645.2 nm was scanned in order to prove applicability of the laser beam source for CH_4-Lidar measurements.

2. LASER MODEL

For modeling the pulsed laser emission, pumping and lasing process are treated independently, which is feasible given their very different time scales (cw-pumping at 100 Hz repetition rate and ns pulse duration). Both pumping and lasing process are modeled in 2.5 dimensions (assuming rotational symmetry with respect to the beam propagation axis). Spatial resolution is established by virtually cutting the laser crystal into 100 segments along the beam propagation direction (z-axis) and another 100 segments along the radial axis (r-axis).
The pumping process takes into account spatially resolved absorption bleaching. For achieving this, the pump duration (which is the inverse repetition rate) is cut into time slices which are shorter by two orders of magnitude than a predicted bleaching time. This bleaching time is estimated as the time required for absorbing the maximal storable pump energy in the laser crystal for a given pump intensity. For each time step, a Gaussian transversal distribution containing the energy content of the time slice at the given slice duration and pump power is propagated through the crystal along the z-axis. In each z-segment of the crystal, absorption of incident the pump energy is computed with radial resolution and the pump energy distribution is reduced by the absorbed amount and propagated to the next z-segment. With the absorbed pump

Updated 1 March 2012

light the new population of the upper pump multiplet is computed, which then is used for modifying the absorption coefficient of each spatial segment for the next time slice. This way, the spatial distribution of the stored energy in the laser crystal at the moment before laser pulse emission is computed. This distribution also reflects its deviation from the Gaussian shape of the incident pump light, which occurs because the ground level is preferably bleached in regions of high pump intensity.

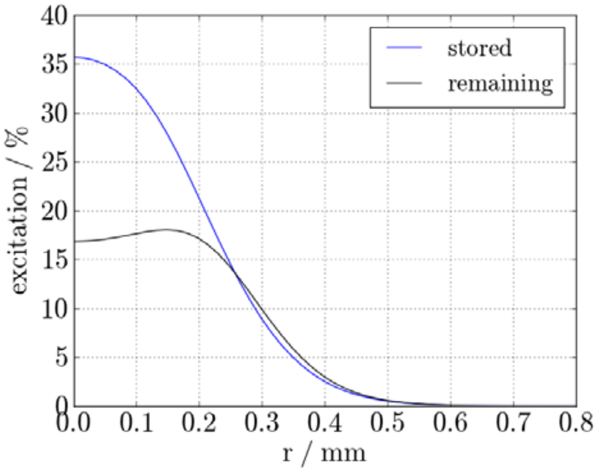

Figure 1. Computed excitation before and after laser pulse extraction.

The laser process is then modeled by solving four coupled rate-equations for the populations of the upper laser multiplet, the upper laser Stark level, the lower laser Stark level and the laser photon density. The solution is obtained with a spatially resolved Runge-Kutta algorithm in fourth order. Gain and loss factors can additionally also be resolved spectrally which results in a spectral output prediction.

As shown in Figure 1, this model allows prediction of the radial distribution of the excitation (fraction of available dopant ions in the upper laser multiplett) before and after laser pulse emission. In Figure 1, the results of such simulations for the laser oscillator described below are depicted.

3. EXPERIMENTAL SETUP

The setup of the laser oscillator is schematically sketched in Figure 2.

The laser crystal, Er:YLuAG, was developed at the Institute for Laser Physics of the University of Hamburg with the method of “compositional tuning” ([4]) as a mixture of Er:YAG and Er:LuAG. The purpose of using this “mixed garnet” crystal was to tune the gain peak of the active medium to the desired emission wavelength of 1645.2 nm in air. The laser crystal had rod geometry with a diameter of 3 mm and a length of 50 mm. It was doped with 0.5 at-% of Erbium and thermally contacted to a passive copper heat sink. Active cooling of the heat sink is foreseen but could not be established to date because of technical issues.

As pump sources, two fiber-laser amplified DFB-diodes were used. Each pump source (in the following, they will be called fiber lasers) provided 4 W of linearly polarized, single-mode cw laser radiation at 1532 nm. The laser crystal was end-pumped from both ends. The waist radius of the pump radiation was 330 µm. This waist was placed inside the laser rod. The pump light entered the laser oscillator through two dichroic pump mirrors which were highly transmittive for the pump light and highly reflective for the laser light at 1645 nm.

The laser resonator consisted of a highly reflective plane end mirror, a partially reflective plane outcoupling mirror (the reflectivity providing the highest output pulse energy was 87 %) and an intracavity spherical lens with a focal length of 227 mm for laser mode shaping. The total physical length of the laser resonator was 410 mm. The thermal lens of the laser crystal let the eigenmode of this laser resonator provide a region of small mode radius close to the outcoupling mirror, where the laser crystal was located. In the laser crystal, an eigenmode radius of 280 µm was achieved. Between the intracavity lens and the end mirror, laser mode radius was considerably higher (about 460 µm). Thus, the risk for laser-induced damage of optical components placed in this region was significantly reduced.

As a Q-switch, a double-RTP Pockels Cell, a quarter wave plate for on-q-switching and a thin film polarizer were placed in the large mode-radius region of the laser resonator. An additional etalon in the laser resonator was used for discrimination of the 1617-nm transition.

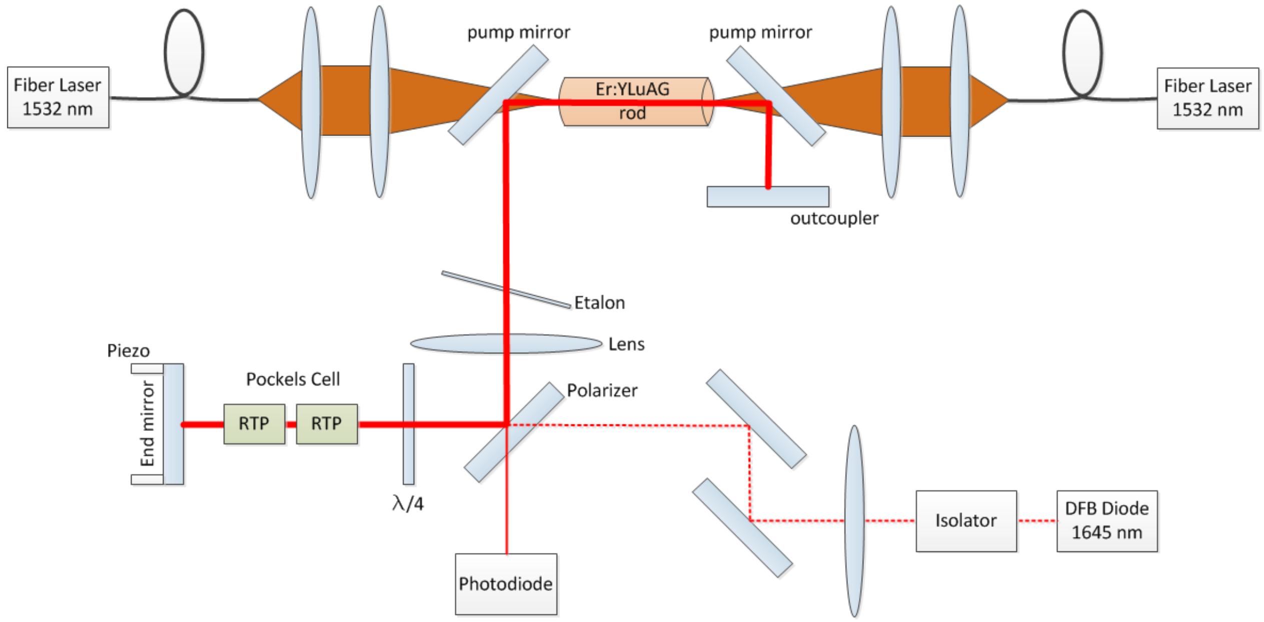

Figure 2. Schematic sketch of the single-frequency laser oscillator.

With this setup, the longitudinal multimode (free running, “fr”) laser experiments were carried out. For single-frequency operation, Ramp-and-Fire method was used. For this, the end mirror was mounted on a piezo ring actor and with this moved several free spectral ranges of the laser resonator within few microseconds prior to emission of each single laser pulse. A cw DFB-diode laser, which could be tuned to any desired emission wavelength in the relevant spectral region between 1644 nm and 1646 nm, was mode-matched to the eigenmode of the laser resonator and coupled into the laser resonator through the thin film polarizer. The Fabry-Perot-interference signal of the diode laser light in the laser resonator was detected with a photodiode. When the photodiode detected a peak of the optical signal, the optical laser resonator length met constructive interference condition of the DFB diode laser wavelength and the Pockels Cell was switched to release a laser pulse.

4. EXPERIMENTAL RESULTS

In Figure 3, the input-output characteristics of the described laser oscillator are shown. The blue curves denote free running mode of operation. The dashed curve shows the measured results, the solid line are the expectations from simulations based on the model described in section 2. The maximum output pulse energy was 3.2 mJ at incident pump power of 7.6 W. This corresponds to an optical efficiency of 4 %. The laser threshold pump power for free running mode of operation was 5.3 W, the slope efficiency was measured to be 17 %. The measured curve showed a roll-over at pump powers above 6.5 W, which is at least not fully thermal, because it was not observed when outcoupling mirrors with lower reflectivities were used.

In single-frequency mode of operation, the pulse energy dropped to 2.3 mJ at 7.6 W of incident pump power. Single-frequency laser pulses could only be measured at pump powers in excess of 7 W. Below this value, increased reabsorption losses in the laser crystal lowered the cavity finesse and deteriorated the Ramp-and-Fire detection signal. Therefore, a laser threshold pump power could not be measured for single-frequency operation.

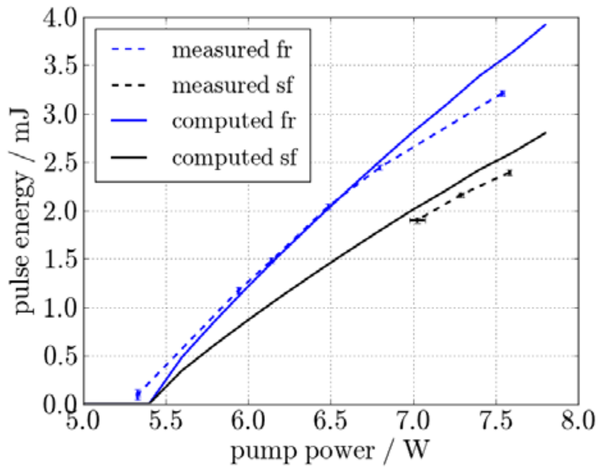

Figure 3. Input-Output Characteristics of the laser oscillator. The results from free running mode are drawn in blue while in black the curves for single-frequency operation are shown. Dashed curves mark measured values while the solid lines are simulation predictions.

The lower pulse energy in single-frequency operation is attributed to spectral hole-burning. Another reason for the pulse energy drop can be deduced from Figure 4, which shows the results of the beam profile and beam propagation factor measurements. On the left hand side, the measured caustic for single-frequency operation is shown. The emission is purely TEM00. This was expected because higher transversal modes have slightly different wavelengths due to the Guoy phase shift and are thus additionally suppressed by Ramp-and-Fire. In free running operation, the beam propagation factor of about $M^2 = 1.3$ reveals some contribution of higher order modes to the transversal beam shape which also increase beam radius and overlap efficiency in the laser crystal, which in turn can lead to higher pulse energy.

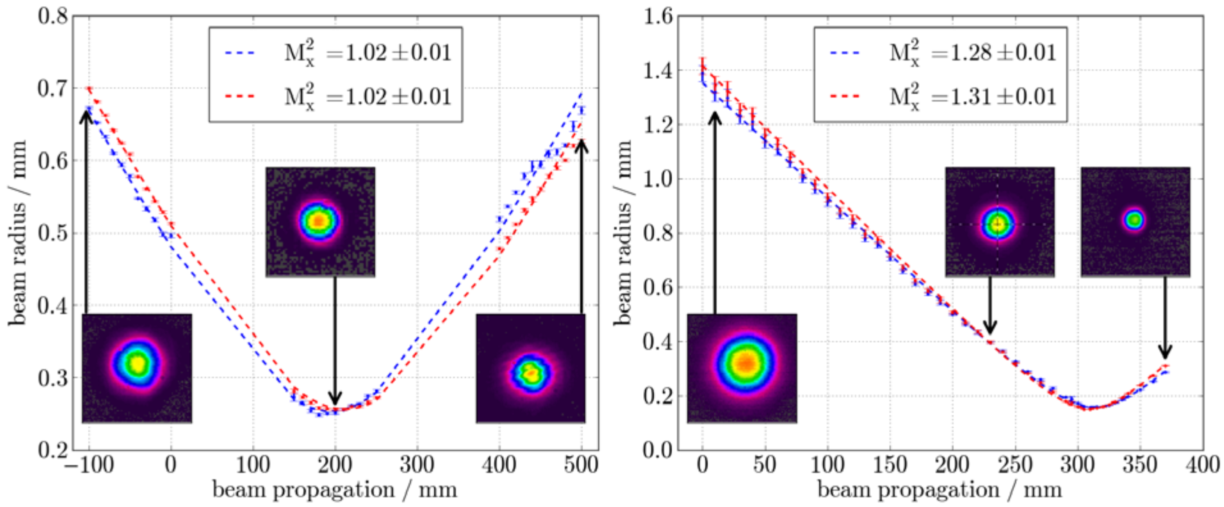

Figure 4. Caustic measurements of the laser emission in single-frequency (left) and free running (right) operation.

The pulse duration was measured to be 84 ns FWHM in both single frequency and free running operation at full pump power. The temporal pulse shapes are depicted in Figure 5. The upper plot shows the profile in free running operation and shows pronounced beating of several present longitudinal resonator modes. In single-frequency operation, the temporal pulse shape is smooth as shown in the lower plot.

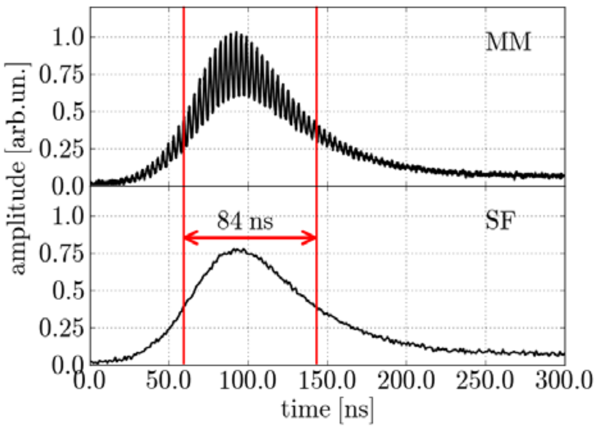

Figure 5. Temporal pulse profile in free running (upper plot) and single-frequency operation (lower plot) measured at full pump power of 7.6 W. The pulse duration was measured to be 84 ns FWHM.

The output spectrum of the laser oscillator in free running operation is shown in Figure 6. The measured spectrum (blue curve) was compared with the result from the spectrally resolved performance model (black curve). The pronounced structures in the spectrum could thus be explained with etalon effects of optical components in the laser resonator (lens, Pockels Cell, outcoupling mirror).

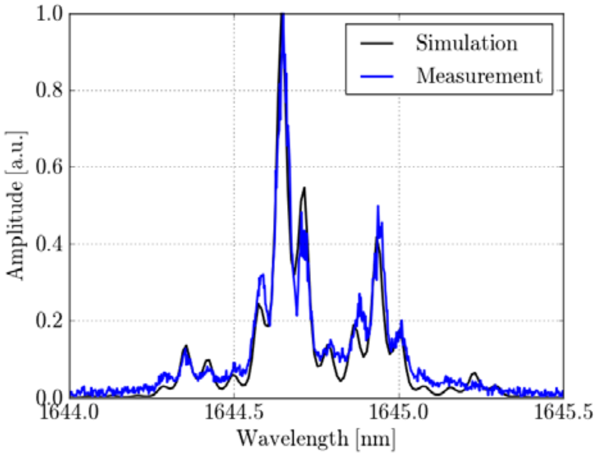

Figure 6. Measured (blue) and simulated (black) laser spectrum in free running q-switched operation. The simulated spectrum was obtained with the described performance model. The pronounced spectral structure is due to etalon effects of the optical components in the laser oscillator.

Stable single-frequency operation at full pump power was achieved in the wavelength range between 1644.3 nm and 1645.4 nm. Wavelength tuning was performed by tuning the wavelength of the seed laser. The tuning curve is shown on the left hand side of Figure 7. The stable single-frequency range is marked in red. The spectral structure of the tuning curve is again due to etalon effects of the optical components in the laser resonator. The CH_4 detection wavelengths (online and offline) for the MERLIN mission are indicated with red lines.

Also shown in blue is the fluorescence curve of the used Er:YLuAG laser crystal. It can be seen, that the composition of the laser crystal is not yet optimal because the gain peak is not located at the MERLIN wavelengths. The right hand side of Figure 7 shows the measured spectral width of 13 000 individual single-frequency laser pulses. This measurement was performed with a heterodyne setup, in which the laser pulses were interfered with a fraction of the seed laser signal after shifting the latter by 200 MHz using an acousto-optic modulator. The resulting beat signal was detected with a fast photo detector. A fast Fourier transform for each pulse was performed to provide the laser pulse spectrum. Spectral widths of 12 MHz were measured, which met the requirements for the MERLIN transmitter.

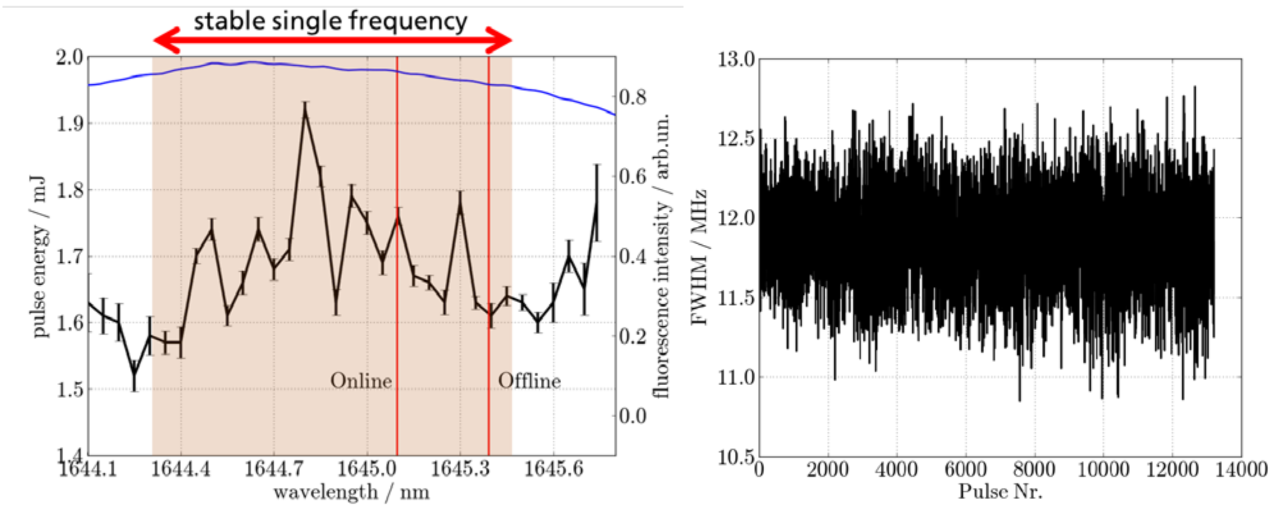

Figure 7. Left: Tuning curve of the single frequency laser. The region marked in red is the spectral region were stable single-frequency operation was observed. The blue curve shows the fluorescence spectrum of the used laser crystal. Right: Spectral width of individual single-frequency laser pulses measured with heterodyne setup.

In order to demonstrate the applicability of the laser oscillator for Lidar measurements, the CH_4 absorption line at 1645.1 nm was scanned. Therefore, a fraction of the laser pulses was directed through a CH_4 gas cell and transmission of the cell for the laser pulses was measured as a function of the seed laser wavelength. The result is shown in Figure 8, together with a prediction of the CH_4 absorption line taken from HITRAN database ([5], red curve). The absorption line with its substructure was resolved in full agreement with the theoretical prediction.

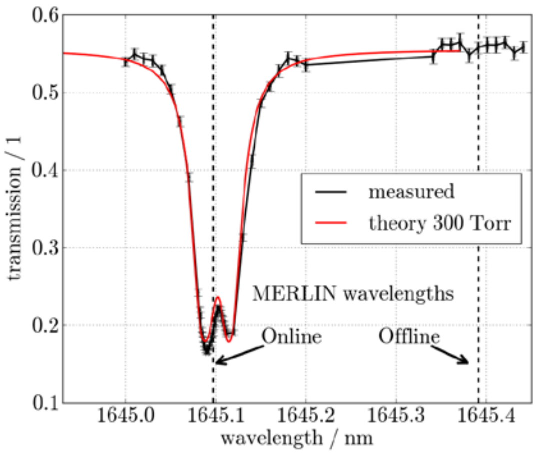

Figure 8. Transmission of a CH_4 gas cell for the laser pulses from the single-frequency laser oscillator. The absorption line at 1645.1 nm and its substructure was resolved in agreement with the theoretical prediction from HITRAN database. [5]

For comparison, a different pumping scheme based on fiber-coupled diode lasers at 1532 nm was tested. The delivery fibers had a NA of 0.22 and a core diameter of 400 µm. A barrel-polished laser rod of diameter 1.2 mm and 25 mm length was end-pumped from both ends with two diode laser modules. The pump light was guided in the laser rod by total internal reflection at the polished barrel surface while the laser mode propagated freely through the laser rod. Such a pumping scheme was reported before for Er:YAG-lasers at 1.6 µm. [6]

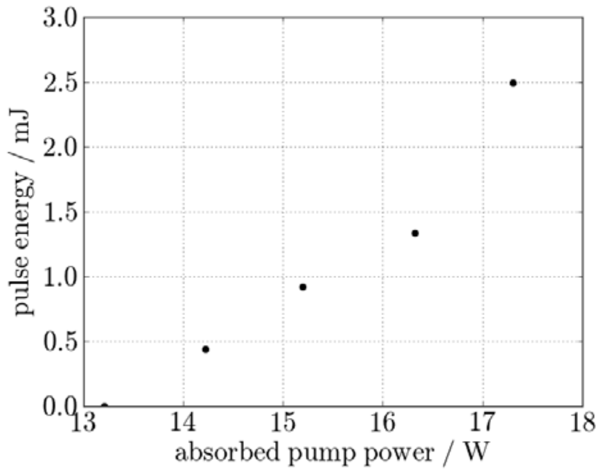

Figure 9. Input-Output characteristics of the laser oscillator with diode laser pumping.

A crystal pumped in this way was tested in the same laser resonator as described above. The attained pulse energy as a function of absorbed pump power is given in Figure 9. The maximal measured pulse energy was 2.5 mJ, the optical efficiency with respect to absorbed pump power was 1.4 %. The low efficiency reflects non-optimal mounting of the laser crystal. Substantial losses at pumping mirrors and at the thin film polarizer give evidence to stress-induced depolarization of the laser mode in the laser crystal.

5. CONCLUSION

A resonantly-pumped single-frequency laser oscillator with Er:YLuAG as active medium was demonstrated. It produced single-frequency laser pulses with 2.3 mJ of energy at a repetition rate of 100 Hz and pulse duration of 90 ns. Stable single-frequency laser pulses were observed in the spectral region between 1644.3 nm and 1645.4 nm. The spectral width of the laser pulses was 12 MHz FWHM, which is suitable for differential absorption Lidar-measurements of CH_4 in the atmosphere. The CH_4-absorption line at 1645.1 nm of CH_4 in a reference gas cell was scanned. The transmission spectrum was in agreement with the data taken from HITRAN database. In free-running mode of operation, pulse energy reached 3.2 mJ and the emission spectrum showed pronounced structure due to etalon effects of optical components in the laser resonator.

A performance model with spatial and spectral resolution was established, which provided prediction that could be experimentally reproduced. This model is based on laser rate equations and included pump light absorption saturation and laser reabsorption. Inclusion of energy transfer effects is foreseen in future work, as is the extension of the radial symmetry to a purely 3-dimensional spatial resolution.

Potential for increasing the efficiency is seen in active water cooling of the laser crystal heat sink and an optimized thermal contact of the laser crystal to the heat sink. Also, the available pump power will doubled in future experiments and an additional INNOSLAB pulse amplifier will be set-up.

Finally, an optimized mounting of the barrel-polished laser rods for experiments with the fiber-coupled diode laser modules as pump sources promises to overcome existing stress-induced birefringence losses and substantially increase the efficiency of this setup.

REFERENCES

[1] UN IPCC, „Third Assessment Report - Climate Change 2001: Synthesis Report," Cambridge University Press, Cambridge, (2001).

[2] Kiemle, C., Quatrevalet, M., Ehret, G., Amediek, A., Fix, A., Wirth, M., "Sensitivity studies for a space-based methane lidar mission", Atmos. Meas. Tech. 4, 2195–2211 (2011).

[3] Löhring, J., Meissner, A., Hoffmann, D., Fix, A., Ehret, G., Alpers, M., "Diode-pumped single-frequency-Nd:YGG-MOPA for water-vapor DIAL measurements: design, setup and performance," Appl Phys B 102, 917-935 (2011).

[4] Barnes, N. P., Murray, K. E., Ertur, E. B., Walsh, B. M., Hutcheson, R. L., "Compositionally Tuned Solid State Lasers" in OSA TOPS on Advanced Solid-State Lasers, Payne, S. A., Pollock, C. (eds.), Optical Society of America, Washington, DC (1996).
[5] Rothman, L. S., et. al., "The HITRAN 2008 molecular spectroscopic database", Journal of Quantitative Spectroscopy & RadiativeTransfer 110, 533–572, (2009).
[6] Eichhorn, M., "Thermal lens effects in an Er^{3+}:YAG laser with crystalline fiber geometry", Appl Phys B 94, 451–457, (2009).